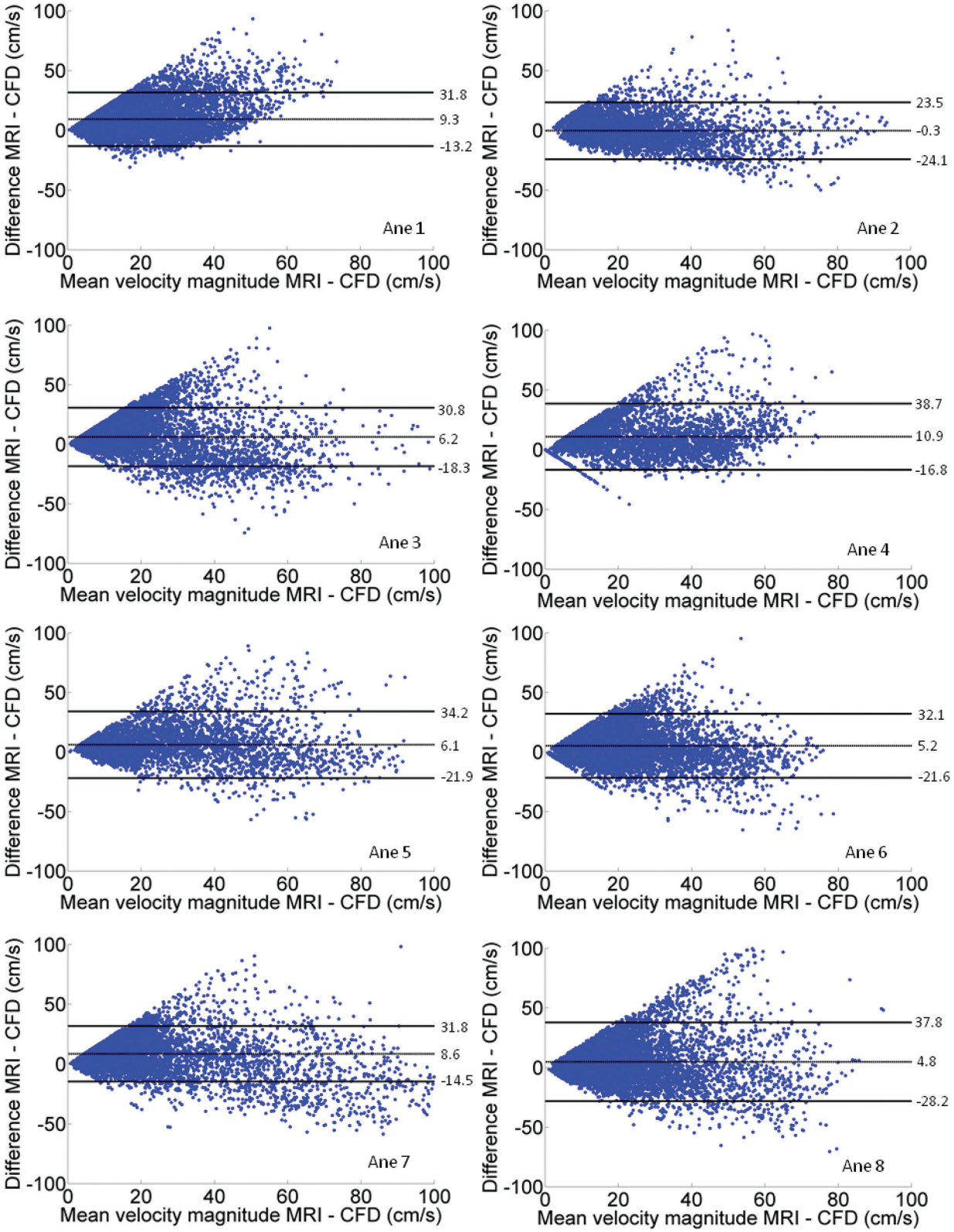

ON-LINE FIG 1. Bland-Altman plots showing the difference between velocity magnitude from 3D PC-MRI and CFD, with inflow boundary conditions obtained from 2D PC-MRI.

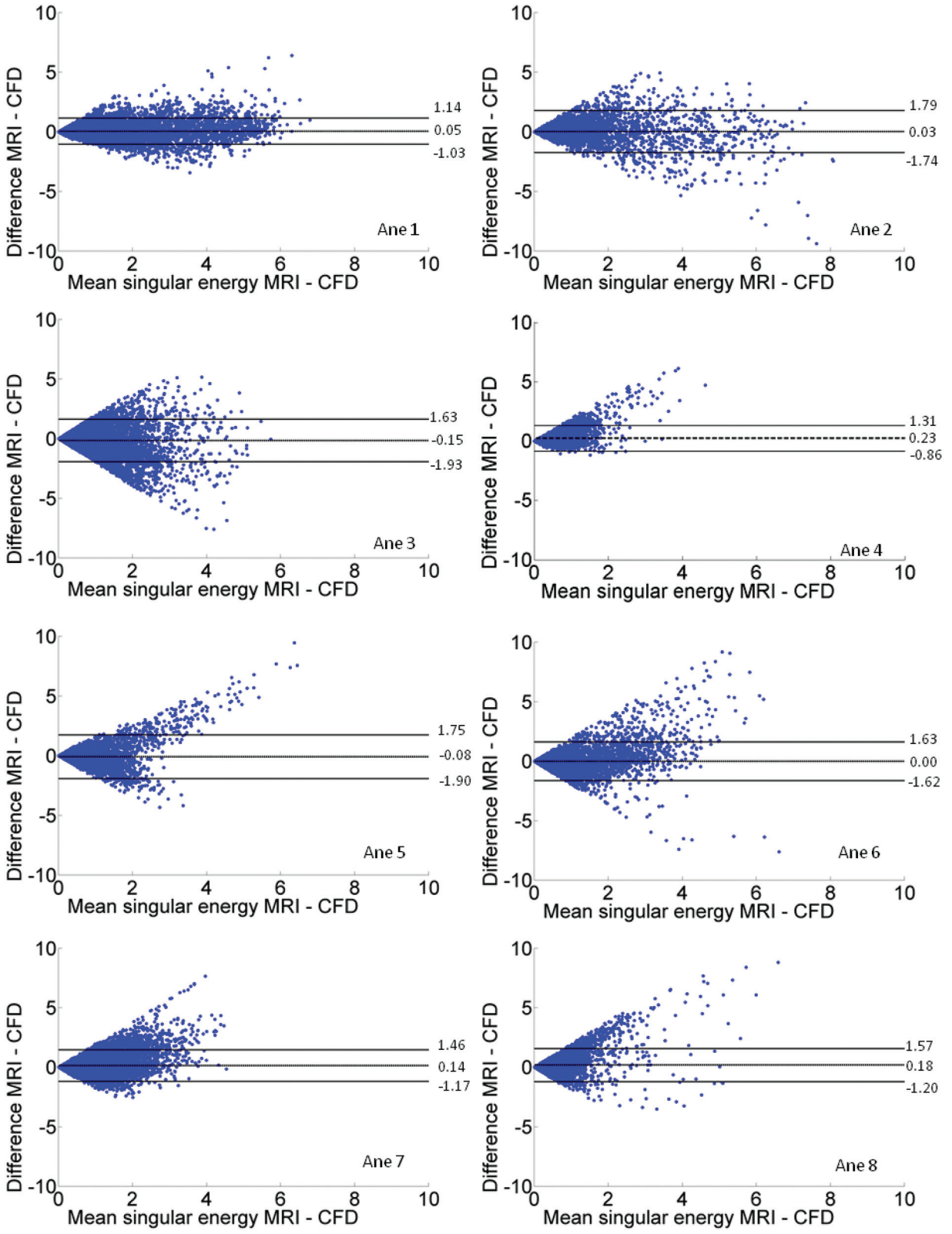

ON-LINE FIG 2. Bland-Altman plots showing the difference between singular energy from 3D PC-MRI and CFD, with inflow boundary conditions obtained from 2D PC-MRI.

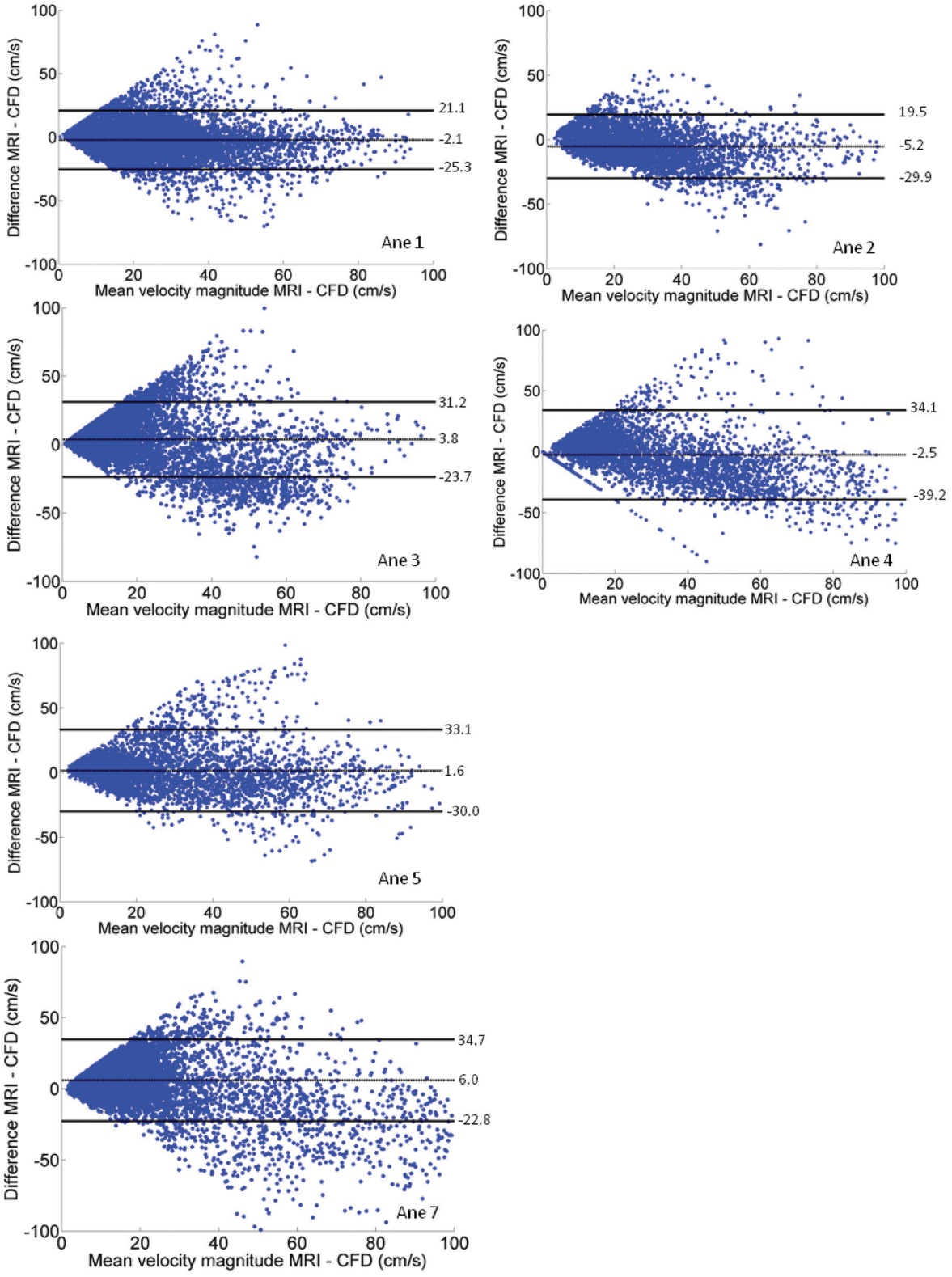

ON-LINE FIG 3. Bland-Altman plots showing the difference between velocity magnitude from 3D PC-MRI and CFD, with inflow boundary conditions obtained from 3D PC-MRI.

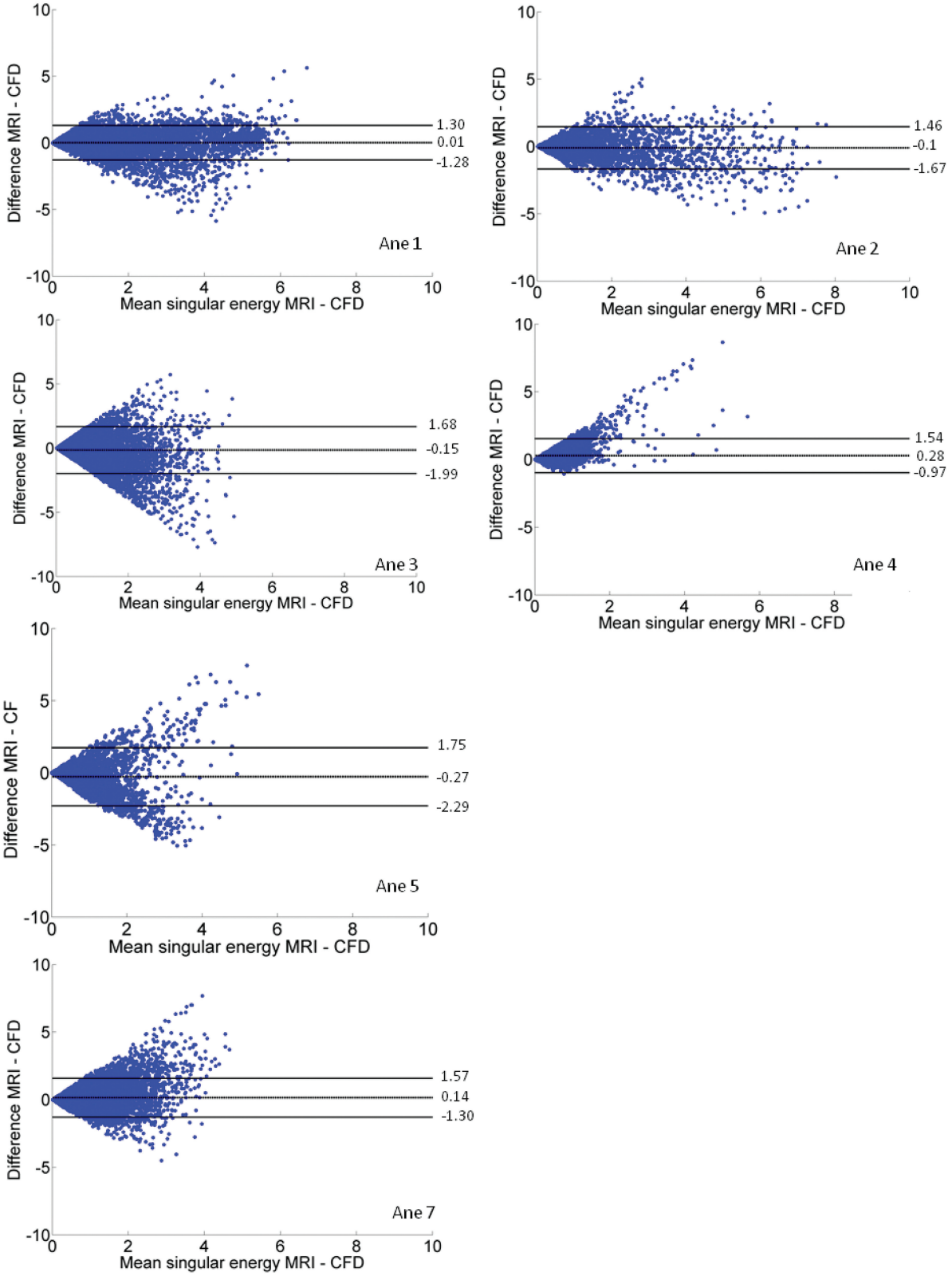

ON-LINE FIG 4. Bland-Altman plots showing the difference between singular energy from 3D PC-MRI and CFD, with inflow boundary conditions obtained from 3D PC-MRI.

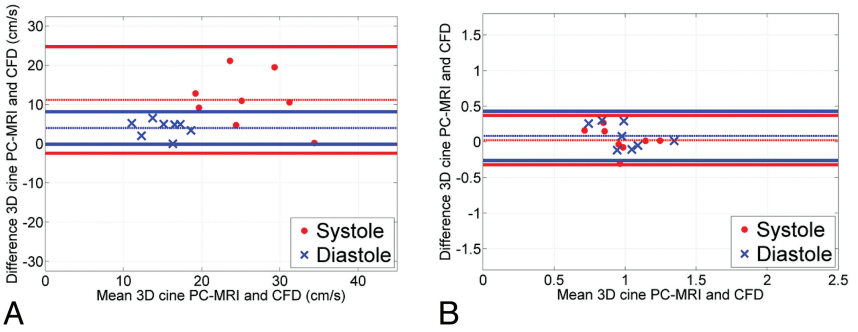

ON-LINE FIG 5. Bland-Altman plots for velocity magnitude (*A*) and singular energy difference (*B*) between 3D PC-MRI and CFD, with inflow boundary conditions obtained from 2D PC-MRI at peak systole and diastole for all aneurysms.

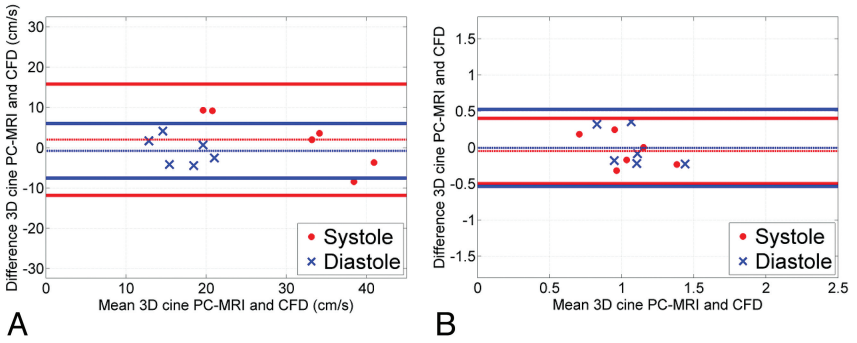

ON-LINE FIG 6. Bland-Altman plots for velocity magnitude (*A*) and singular energy difference (*B*) between 3D PC-MRI and CFD, with inflow boundary conditions obtained from 3D PC-MRI at peak systole and diastole for all aneurysms.

On-line Table 1: Locations and size of the aneurysms, voxel size of the 3D rotational angiography datasets, volumes, number of elements, element density of the meshes and input flows, inflow vessel areas, mean velocity magnitude, and peak systolic velocity as measured by 2D and 3D PC-MR imaging

Aneurysm	Location	Size (mm, length × width × height)	Isotropic Voxel Size 3D RA (mm^3)	Mesh Volume (mm^3)	No. of Mesh Elements	Element Density (elements/mm^3)	Input Flow (mL/s)		Inflow Vessel Area (mm^2)		Input Mean Velocity Magnitude (cm/s)		Input Peak Systolic Velocity (cm/s)	
							2D	3D	2D	3D	2D	3D	2D	3D
1	Left MCA	12.6 × 7.3 × 9.1	0.22	554	1.765.310	3186	1.7[a]	3.4[a]	5.9[a]	10.5[a]	31[a]	35[a]	89[a]	86[a]
2	BA	7.4 × 6.2 × 6.4	0.22	272	1.422.476	5230	2.2	3.1	5.3	11.9	41	27	87	95
3	Right MCA	13.0 × 7.9 × 11.3	0.25	732	2.608.270	3563	2.0	3.8	3.6	10.2	57	39	111	110
4	Right MCA	5.6 × 5.0 × 7.2	0.10	261	1.467.689	5623	2.2	3.5	6.3	12.8	37	29	78	110
5	Right MCA	9.2 × 6.0 × 5.3	0.17	260	1.168.002	4492	1.9	3.2	4.0	10.3	49	31	102	99
6	BA	8.8 × 8.7 × 11.5	0.22	588	2.313.009	4282	2.1[b]	2.2[b]	6.9[b]	9.4[b]	31[b]	25[b]	69[b]	78[b]
7	Left MCA	12.0 × 12.1 × 9.7	0.22	674	2.238552	3934	2.3	2.8	4.6	10.3	52	29	123	106
8	BA	10.3 × 9.3 × 10.9	0.22	687	2.559.296	3725	2.6[b]	2.9[b]	6.0[b]	12.6[b]	44[b]	24[b]	87[b]	89[b]

Note:—BA indicates basilar artery.

[a] The 2D PC-MR scan was obtained in the coiled aneurysm, 10 months after the 3D PC-MR scan of the uncoiled aneurysm.

[b] It was not possible to measure flow at the same locations because the 2D PC-MR was performed outside the imaging volume of the 3D PC-MR measurement.

On-line Table 2: Differences between velocity fields as determined with 3D PC-MRI and CFD with boundary conditions obtained from 2D PC-MRI for the dome of the aneurysm and the inflow vessel[a]

No.	*MDif* (cm/s)				*SDif* (%)				*RDif* (%)			
	Systole		Diastole		Systole		Diastole		Systole		Diastole	
	Dome	Inflow	Dome	Inflow	Dome	Inflow	Dome	Inflow	Dome	Inflow	Dome	Inflow
1	17.9	39.5	1.1	5.3	11.2	14.1	5.0	6.4	167.9	133.9	11.7	21.8
2	−0.8[b] ($P = .32$)	9.2	−1.1	5.9	14.2	23.1	7.6	9.2	2.7	17.7	7.6	26.5
3	12.5	18.7	5.8	7.1	11.8	18.5	6.8	7.3	183.2	33.2	106.5	24.5
4	16.5	25.0	6.3	1.4	10.3	22.5	6.7	12.4	270.1	59.2	103.1	4.6
5	6.2	18.7	1.4	6.3	13.8	24.9	8.1	17.1	41.9	39.5	12.6	21.4
6	5.7	7.5	6.0	4.0	10.9	13.5	12.8	10.6	31.3	16.1	14.0	14.7
7	12.6	17.3	7.1	2.0	8.5	27.7	8.5	20.3	166.4	95.5	28.7	5.3
8	10.2	9.3	5.4	4.3	14.1	21.8	13.0	10.7	77.9	19.1	51.1	18.9

[a] Indicated are *MDif*, *SDif*, and *RDif*, as determined on a voxel basis.

[b] Nonsignificant difference.

On-line Table 3: Differences between velocity fields as determined with 3D PC-MRI and CFD[a]

	MDif (cm/s)				*SDif* (cm/s)				*RDif* (%)				Median Angle (°)			
	Systole		Diastole		Systole		Diastole		Systole		Diastole		Systole		Diastole	
Aneurysm	2D BC	3D BC	2D BC	3D BC	2D BC	3D BC	2D BC	3D BC	2D BC	3D BC	2D BC	3D BC	2D BC	3D BC	2D BC	3D BC
1	21.1	1.9	2.0	−4.2	12.7	17.0	6.3	8.1	161.8	6.0	17.8	23.9	20.6	20.8	26.5	27.8
2	0.2[b] ($P = .77$)	−8.5	−0.0[b] ($P = .97$)	−4.5	17.1	16.9	8.5	9.7	0.6	19.9	0.1	21.5	16.9	18.5	24.7	25.5
3	9.2	9.2	5.2	1.6	18.0	17.8	9.6	12.0	61.0	61.4	62.1	13.7	37.3	33.3	52.6	50.7
4	19.5	−3.7 ($P = .002$)	4.9	−2.6	17.9	26.3	10.2	12.8	99.6	8.7	33.4	11.5	26.3	24.0	30.3	31.0
5	10.5	3.5	3.4	0.7[b] ($P = .21$)	17.2	19.3	10.9	11.9	40.6	10.8	20.0	3.5	21.1	22.0	25.5	27.5
6	4.8	–	4.8	–	14.2	–	12.2	–	21.6	–	34.3	–	27.2	–	48.4	–
7	12.8	9.1	6.5	4.0	12.0	16.9	10.4	13.4	100.1	56.0	62.6	32.2	32.2	37.3	44.1	49.1
8	10.9	–	5.0	–	19.8	–	13.0	–	55.7	–	39.3	–	34.4	–	49.7	–
Average	11.1 ± 6.9	1.9 ± 7.0	4.0 ± 2.1	−0.8 ± 3.5	16.1 ± 2.8	19.0 ± 3.7	10.1 ± 2.1	11.3 ± 2.0	67.6 ± 51.4	27.1 ± 24.9	33.7 ± 21.5	17.7 ± 10.2	27.0 ± 7.2	26.0 ± 7.5	37.7 ± 12.1	35.3 ± 11.5

Note:—2D BC indicates the CFD simulations with inflow boundary conditions from 2D PC-MRI; 3D BC, CFD with inflow boundary conditions obtained from 3D PC-MRI; –, not possible to perform the CFD with inflow boundary condition obtained from 3D PC-MRI because the CFD inflow boundary was located outside the imaging volume of the 3D PC-MRI measurement.

[a] Indicated *MDif*, *SDif*, and *RDif* and the median angle as determined on a voxel basis and averaged over the whole aneurysm and connecting vessels, between 3D PC-MRI and CFD.

[b] Nonsignificant difference. All *P* values not given were $P < .0001$.

On-line Table 4: Differences between singular-energy fields as determined with 3D PC-MRI and CFD[a]

	MDif				*SDif*				*RDif* (%)			
	Systole		Diastole		Systole		Diastole		Systole		Diastole	
Aneurysm	2D BC	3D BC	2D BC	3D BC	2D BC	3D BC	2D BC	3D BC	2D BC	3D BC	2D BC	3D BC
1	0.02[b] ($P = .42$)	0.00[b] ($P = .93$)	−0.05 ($P = .001$)	−0.09	0.66	0.67	0.55	0.74	1.3	0.1	4.4	7.5
2	0.02[b] ($P = .55$)	−0.23	0.01[b] ($P = .74$)	−0.23	0.64	0.79	1.01	1.06	1.3	15.6	1.1	14.7
3	−0.08 ($P = .0007$)	−0.17	−0.11 ($P = .002$)	−0.22	0.83	0.93	1.24	1.41	7.6	15.3	9.7	18.2
4	0.16	0.18	0.30	0.32	0.60	0.51	1.12	1.18	25.6	29.6	43.8	47.6
5	−0.04[b] ($P = .37$)	−0.32	−0.12 ($P = .0003$)	−0.18	0.91	0.94	0.75	0.97	3.6	28.5	11.6	17.4
6	−0.31	–	0.08 ($P = .015$)	–	0.97	–	0.94	–	27.4	–	8.2	–
7	0.15	0.24	0.29	0.35	0.57	0.86	1.08	1.11	19.1	29.2	34.6	39.6
8	0.27	–	0.26	–	0.79	–	0.76	–	37.8	–	41.7	–
Average	0.02 ± 0.17	−0.05 ± 0.23	0.08 ± 0.18	−0.01 ± 0.27	0.75 ± 0.15	0.78 ± 0.17	0.93 ± 0.23	1.08 ± 0.22	15.5 ± 13.9	19.7 ± 11.7	19.4 ± 17.6	24.2 ± 15.7

Note:—2D BC indicates the CFD simulations with inflow boundary conditions from 2D PC-MRI; 3D BC, CFD with inflow boundary conditions obtained from 3D PC-MRI; –, not possible to perform the CFD with inflow boundary condition obtained from 3D PC-MRI because the CFD inflow boundary was located outside the imaging volume of the 3D PC-MRI measurement.

[a] Indicated are *MDif*, *SDif*, and *RDif*, and the median angle, as determined on a voxel basis and averaged over the whole aneurysm and connecting vessels, between 3D PC-MRI and CFD.

[b] Nonsignificant difference. All *P* values not given were $P < .0001$.